THE JOURNAL OF BIOLOGICAL CHEMISTRY VOL. 284, NO. 34, pp. 22736–22746, August 21, 2009

Mechanism for HIV-1 Tat Insertion into the Endosome Membrane*[S]

Received for publication, May 21, 2009 Published, JBC Papers in Press, June 23, 2009, DOI 10.1074/jbc.M109.023705

Hocine Yezid[‡], Karidia Konate[§], Solène Debaisieux[‡], Anne Bonhoure[‡], and Bruno Beaumelle[‡1]

From the [‡]Centre d'Etudes d'Agents Pathogènes et Biotechnologies pour la Santé, UMR 5236 CNRS, Université Montpellier II, 34095 Montpellier and the [§]Centre de Recherche en Biochimie Macromoléculaire, UMR 5237 CNRS, 1919 Route de Mende, 34293 Montpellier, France

The human immunodeficiency virus, type 1, transactivating protein Tat is a small protein that is strictly required for viral transcription and multiplication within infected cells. The infected cells actively secrete Tat using an unconventional secretion pathway. Extracellular Tat can affect different cell types and induce severe cell dysfunctions ranging from cell activation to cell death. To elicit most cell responses, Tat needs to reach the cell cytosol. To this end, Tat is endocytosed, and low endosomal pH will then trigger Tat translocation to the cytosol. Although this translocation step is critical for Tat cytosolic delivery, how Tat could interact with the endosome membrane is unknown, and the key residues involved in this interaction require identification. We found that, upon acidification below pH 6.0 (*i.e.* within the endosomal pH range), Tat inserts into model membranes such as monolayers or lipid vesicles. This insertion process relies on Tat single Trp, Trp-11, which is not needed for transactivation and could be replaced by another aromatic residue for membrane insertion. Nevertheless, Trp-11 is strictly required for translocation. Tat conformational changes induced by low pH involve a sensor made of its first acidic residue (Glu/Asp-2) and the end of its basic domain (residues 55–57). Mutation of one of these elements results in membrane insertion above pH 6.5. Tat basic domain is also required for efficient Tat endocytosis and membrane insertion. Together with the strict conservation of Tat Trp among different virus isolates, our results point to an important role for Tat-membrane interaction in the multiplication of human immunodeficiency virus type 1.

The human immunodeficiency virus, type 1 (HIV-1),[2] transactivating protein Tat is a small basic protein of 86–102 residues, depending on the viral isolate (1). An essential function of this protein is to participate in the transcription of viral genes. In the absence of Tat, transcription from the HIV-1 long terminal repeat only produces short RNA, whereas the expression of Tat results in the production of long RNA and a marked increase in gene expression (2). Tat is also involved in other steps enabling virus production and is strictly required for HIV-1 multiplication within infected cells (2).

A number of studies suggest that Tat function is not restricted to infected cells (1, 3–7). Indeed, the infected cells secrete Tat (3) using a secretion process that is termed unconventional, because Tat does not have a signal sequence. Accordingly, Tat secretion is insensitive to the fungal metabolite brefeldin A, indicating that Tat bypasses the endoplasmic reticulum to exit the cell (8). This is the case for most proteins secreted using nonclassical secretion mechanisms (9). Although some of these pathways have been characterized (10), this is not the case for Tat.

Tat concentrations measured in the sera of patients infected with HIV-1 were in the nanomolar range (11). These values are most likely underestimated because Tat binds very efficiently to several cell types, such as endothelial cells (12). Circulating Tat does not seem to result from the lysis of infected cells that instead appear to actively secrete large amounts of Tat into the bloodstream (3). Extracellular Tat can exert different effects on cell functions and generate a wide array of cell responses ranging from cell activation (T-cells and endothelial cells) to stimulation of cytokine secretion (T-cells and monocytes) and cell death (neurons and endothelial and T-cells) (1, 4–7). Accumulating evidence suggests that extracellular Tat is involved in the evolution to AIDS (1, 4–6), and Tat is considered as an important component in developing anti-HIV-1 vaccines (13).

To elicit cell responses, at least on T-cells and monocytes, Tat needs to reach the cytosol (14–16). To this end, Tat first binds to several cellular receptors such as CD26 (17), CXCR4 (11), heparan sulfate proteoglycans (18), and the low density lipoprotein receptor-related protein (19). Tat is then endocytosed (20, 21), essentially by the clathrin-coated pit pathway (15). Once in the endosome, Tat crosses the membrane to enter the cytosol. This translocation step is triggered by endosomal low pH (pH 5.3–5.5) and is facilitated by the cytosolic chaperone Hsp90 (15). Hence, Tat enters cells using a "conventional" endosomal translocating toxin strategy, just like diphtheria toxin, which is the best characterized example of this type of toxin (22). The study of the translocation process of endosome-translocating toxins was facilitated by their ability to insert into model membranes upon acidification (23, 24). Whether Tat is also able to do so has yet to be demonstrated.

Moreover, although the implication of each Tat residue in transcriptional activity has been thoroughly determined (25),

* This work was supported by the CNRS and by grants from the Agence Nationale de Recherches sur le SIDA and Sidaction.
[S] The on-line version of this article (available at http://www.jbc.org) contains supplemental Table 1.
[1] To whom correspondence should be addressed: UMR 5236 CNRS, Case 100, Université Montpellier 2, 34095 Montpellier Cedex 05, France. Tel.: 33-467-14-33-98; Fax: 33-467-14-33-38; E-mail: bruno.beaumelle@univ-montp2.fr.
[2] The abbreviations used are: HIV-1, human immunodeficiency virus, type 1; 10-DN, 10-doxylnonadecane; SUV, small unilamellar vesicles; PEA, *Pseudomonas* exotoxin A; PTD, protein transduction domain; Tf, transferrin; PC, phosphatidylcholine; PG, phosphatidylglycerol; LTR, long terminal repeat.

the molecular determinants that enable Tat to enter the cytosol of mammalian cells has yet to be identified. The Tat basic domain (residues 49–57) is likely involved in cell binding because the corresponding peptide recognizes cell surface heparan sulfate proteoglycans (26, 27), just like native Tat (18). From its capacity to introduce attached proteins into the cell cytosol, this peptide has been termed the protein transduction domain (PTD), and Tat-PTD is a popular tool to deliver cargos intracellularly (28). Tat-PTD has been shown to enter cells using either macropinocytosis (29) or clathrin-mediated endocytosis (30). The fact that Tat and Tat-PTD share a common receptor and can both undergo clathrin-dependent uptake indicates that these early steps of Tat entry into cells might involve the PTD. Whether this is the case for later events such as transmembrane transport is unknown.

A key step in Tat translocation is Tat insertion into the endosome membrane. It is not clear how such a small protein as Tat, which is devoid of a hydrophobic α-helix (31), could undergo membrane insertion. Nevertheless, we previously showed that insertion of *Pseudomonas* exotoxin A (PEA) into the endosome membrane relies on a key tryptophan residue that becomes exposed at endosomal pH (pH 5.3–5.5) and then triggers membrane insertion (24). Other proteins such as annexin-V (32) and protein kinase C-α (33) also undergo such regulated Trp-mediated membrane insertion, although in that case the stimulus triggering insertion is a rise in Ca^{2+} concentration and not acidification. Interestingly, Tat has a single Trp that, despite the high HIV-1 mutation rate (34), is one of the best conserved Tat residues (35). According to a three-dimensional structure based on two-dimensional NMR experiments, Trp-11 is located in the center of the molecule, sandwiched between the core and glutamine-rich domains (31), and is therefore potentially involved in Tat insertion into the endosome membrane.

All known proteins whose membrane insertion is based on a Trp side chain have a molecular device that induces Trp exposure and thereby controls insertion (24, 32, 33). Because the Tat membrane insertion process only takes place within endosomes (15), if Tat actually belongs to this group of proteins it likely possesses a low-pH sensor able to trigger Trp exposure upon endosomal delivery.

Here we showed that Tat inserts into model membranes upon acidification, and we identified key determinants of this insertion process. We found that Tat uses a low-pH sensor involving Asp/Glu-2 and the basic domain to regulate exposure of its single Trp that allows Tat to initiate membrane insertion.

EXPERIMENTAL PROCEDURES

Materials—Chemicals were from Sigma, and phospholipids were from Avanti Polar Lipids. 10-DN was kindly provided by Erwin London (Stony Brook University, New York). Transferrin (Tf) was labeled with Cy5 using the protocol provided by the manufacturer of the labeling kit (GE Healthcare). Monoclonal antibodies were from Advanced Biotechnology Inc. (anti-Tat) and the Iowa Developmental Studies Hybridoma Bank (anti-Lamp-1). Secondary antibodies were obtained as indicated (15).

Cells and Plasmids for Tat Expression and Purification—Jurkat T-cells (clone E6–1) were from ATCC and transfected using electroporation (15). We used a Tat (BH10 isolate) of 86 residues. An elongated version of 101 residues, obtained by mutating the stop codon into Ser (25), was also used for some assays with similar results. Site-directed mutagenesis of Tat in pET-11d vector (for expression in *Escherichia coli*) and pBi-GL (for expression in mammalian cells) was performed using QuikChange kits (Stratagene) and appropriate primers. All mutant DNA coding sequences were entirely sequenced (Genome Express, Meylan, France). Recombinant Tat or Tat mutants were expressed and purified from *E. coli* as described (15), and identification was confirmed by mass spectrometry (Proteomic Facilities of the IFR3, Montpellier, France).

Lipid Vesicles and Fluorescence Spectroscopy—An SS35 spectrofluorometer and ultramicro-quartz 200-μl cuvettes (PerkinElmer Life Sciences) were used. Slit widths were 7 nm for both excitation and emission. Fluorescence intensity was measured at 351 nm using excitation at 279 nm. The background intensity measured in the absence of Tat was subtracted. To prepare small unilamellar vesicles (SUV), lipids (dioleoylphosphatidylcholine (PC)/dioleoylphosphatidylglycerol (PG) 75/25) were dried under N_2 and further dried under high vacuum overnight. The dried lipids were then suspended in 100 mM NaCl, 50 mM citrate, pH 7.2 (citrate buffer), and sonicated using a bath sonicator for 1 h and then a microtip sonicator for 3 min. The resulting SUV had a diameter of 100–200 nm. To prepare brominated vesicles, half of the PC was replaced by 1,2-(9,10-dibromo)stearoyl phosphatidylcholine (24). When indicated the 10-DN quencher was added at 10 mol % before drying the lipids (36). Experiments were performed using 2 μM Tat in citrate buffer, pH 7.0, unless otherwise stated. SUV were used at a concentration of 400 μM lipids. Quencher and SUV concentrations were high enough to produce a minimal dilution that was taken into account for calculation. The inner filter effect caused by the highest acrylamide concentrations was negligible and was not corrected (37).

Monolayer Measurements—Tat insertion into a phospholipid monolayer of PC/PG (75/25) was measured at 23 °C by monitoring the change in surface pressure (π) at constant surface area using a 10-ml square Teflon trough and a small diameter wire probe fitted on a Kibron microtrough S instrument (38). The lipid monolayer was spread onto the citrate buffer subphase until the desired initial surface pressure (π_0) was reached. After 15 min, Tat (26 nM) was injected into the subphase. Following pressure stabilization (15–20 min), the pH was lowered to pH 5.3 by injecting concentrated HCl over a 1-min period. The increase in surface pressure ($\Delta\pi$) was monitored for 30 min while stirring the subphase at 60 rpm. Typically, the $\Delta\pi$ value reached a maximum after 20 min. The resulting $\Delta\pi$ was plotted *versus* π_0, allowing us to determine the critical surface pressure (π_C) as the *x*-intercept (38). For conversion, 1 dyne = 1 mN/m. The statistical significance of the data was examined using the correlation coefficient test.

Transactivation Assays—To examine the capacity of exogenous Tat to enter cells and transactivate the LTR, Jurkat T-cells (9.10^6) were cotransfected with 7 μg of pGL3-LTR, which expresses firefly luciferase under control of the Tat-activated HIV-1-LTR promoter, and 1 μg of pRL-TK (Promega), which codes for *Renilla* luciferase under control of the herpes simplex virus thymidine kinase promoter and is used to normalize

results. After 18 h, 200 nM recombinant Tat (or Tat mutant) and 100 μM chloroquine were added. One day later, cells were lysed for dual luciferase assays (Promega), and transactivation activity was calculated using the firefly/*Renilla* activity ratio (15).

To assess whether Tat mutants preserved a native and reactive structure, Jurkat cells were cotransfected with the luciferase plasmids together with a Tat expression vector (3 or 10 μg, as indicated). After 48 h, cells were lysed, and transactivation activity was determined as described above.

Immunofluorescence—Jurkat T-cells were incubated for 6 h with 50 nM Tat. Tf-Cy5 (100 nM) was added for the last 40 min of labeling. Cells were then washed, fixed with 3.7% paraformaldehyde, processed for Tat and Lamp-1 detection as described (15), and finally viewed under a Leica SPE confocal microscope.

To quantify Tat colocalization with transferrin and Lamp-1 that are early and late endosome markers, respectively, we used images from 20 to 30 cells and the Metamorph software (Universal Imaging). To assess Tat endocytosis efficiency, the same images were used. Tf and Lamp-1 images were summed using Adobe Photoshop, and Tat internalization efficiency (%) was calculated using Metamorph as the percentage of Tat pixels present within a Lamp-1 or transferrin-positive compartment. Visual examination of processed images confirmed that Tat staining outside these structures localized to the plasma membrane. The anti-Tat monoclonal antibody we used for immunofluorescence binds to the first nine residues of Tat. It poorly recognized Tat-E2A and Tat-D5A, and endocytosis of these mutants could therefore not be reliably quantified.

RESULTS

Low pH Induces Tat Conformational Changes—Structural studies of HIV-1 Tat performed by two-dimensional NMR suggested that the Tat single Trp is located within a valley and that Trp fluorescence should be highly sensitive to conformational modifications (31). To assess whether Tat conformation changes upon solvent acidification, we monitored the effect of pH on Tat Trp fluorescence, first in the absence of membrane. Although fluorescence intensity decreased almost linearly with pH, there was nevertheless a small plateau between pH 5.8 and pH 5.5 indicating that a conformational change might take place within this pH range (Fig. 1*A*). Conformational modifications can also be detected by a shift in the wavelength of maximum emission (λ_{max}). We thus monitored whether acidification induced modifications of the ratio of emission intensity at 330 nm to that at 350 nm, a method that is recognized as more accurate than direct measurements of minute λ_{max} shifts (37). The 330/350 ratio increased from pH 7 to pH 4 (Fig. 1*B*), indicating a blue shift in Trp fluorescence. Hence, the Tat Trp environment changes upon acidification. We used fluorescence quenchers to examine whether this environment modification was associated with structural changes leading to enhanced Trp accessibility. Whereas the large ions I^- and Cs^+ failed to reveal a difference in Trp access (Fig. 2, *A* and *B*), acrylamide quenching was more efficient at low pH (Fig. 2*C*). Hence, acidification enabled this small and neutral molecule to reach Tat Trp more easily. This indicates that Tat structure in this region opens when pH drops from pH 7.0 to pH 5.3, and that Tat Trp has easier access to the solvent at pH 5.3. It should be noted that

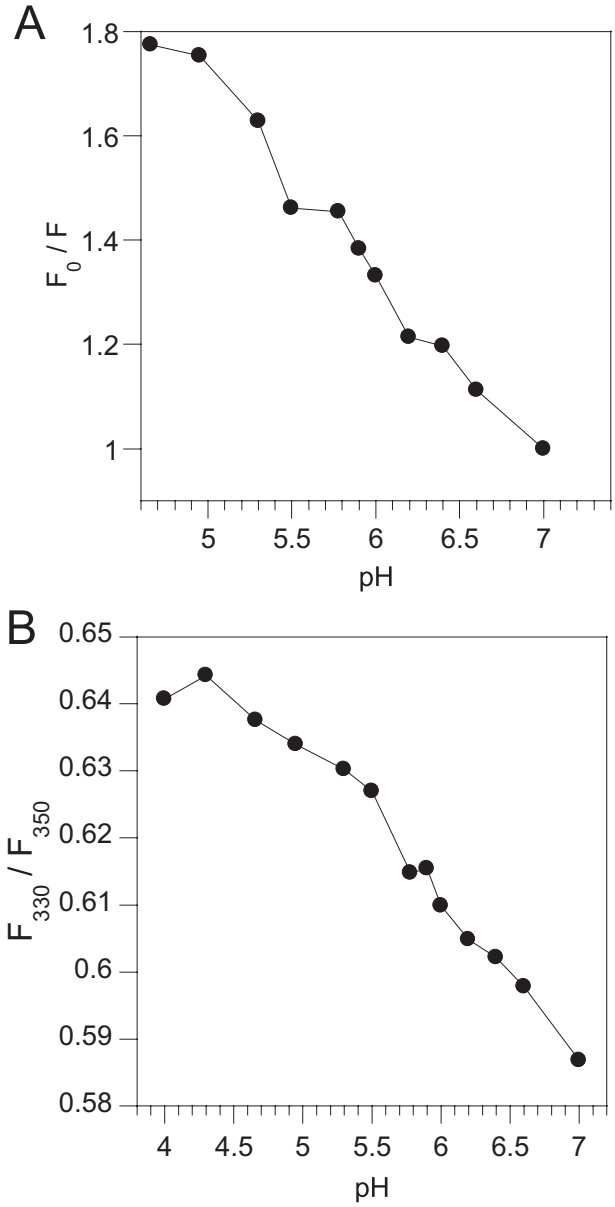

FIGURE 1. **Effect of pH on the Trp fluorescence of Tat in the absence of membrane.** *A,* fluorescence decreases upon acidification. Samples contained 2 μM Tat in 150 mM NaCl, 50 mM citrate (citrate buffer) at the indicated pH. F_0/F is the ratio of fluorescence intensity at pH 7.0 relative to that at the indicated pH. *B,* emission maximum shift as monitored by the ratio of fluorescence intensity at 330 nm to that at 350 nm. The increase in this ratio as the pH dropped denotes a blue shift. Representative results of triplicate experiments are shown.

the latter value is within the endosome pH range (40), and that this molecular reorganization is therefore likely biologically relevant.

Acidification Induces Tat Insertion into Membrane Monolayers—Tat undergoes acid-triggered translocation across the endosomal membrane (15), but it has yet to be shown whether it could insert into model membranes at low pH. To examine this issue, we first monitored the capacity of Tat to penetrate membrane monolayers of dioleoylphosphatidylcholine/dioleoylphosphatidylglycerol (75/25). They were spread at constant area and at an initial surface pressure (π_0) onto a subphase at neutral pH. The change in surface pressure ($\Delta\pi$) was monitored

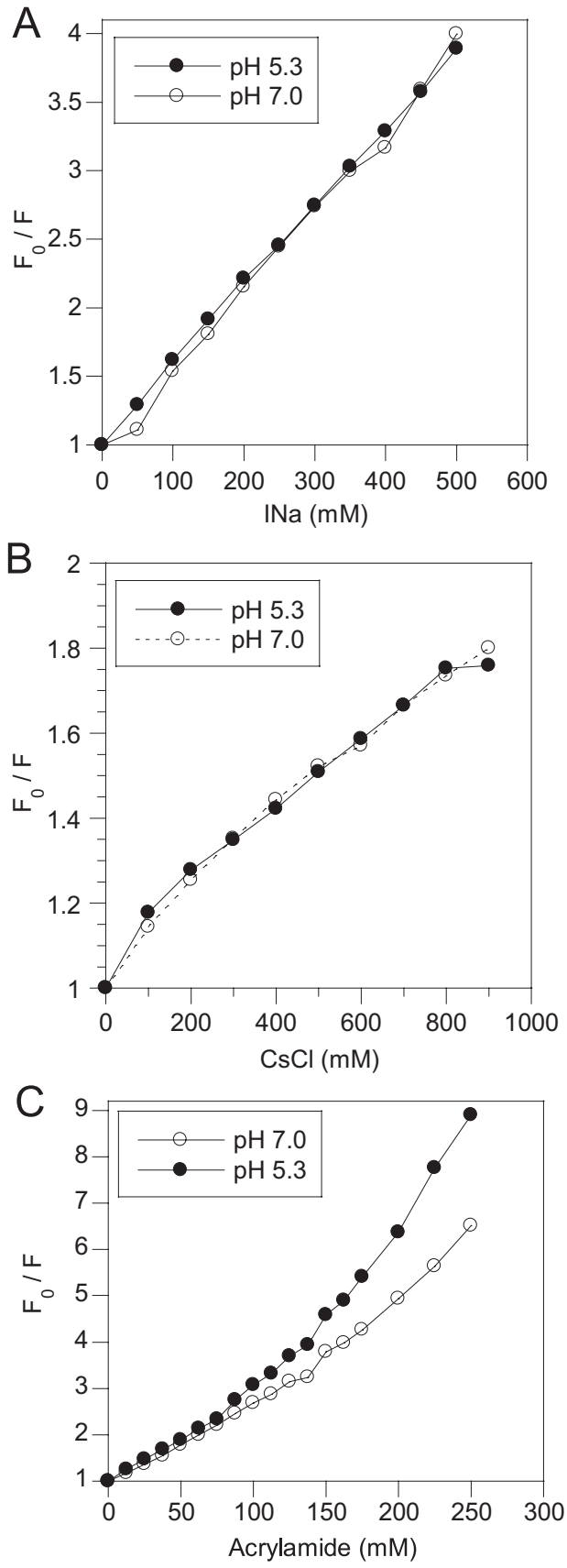

FIGURE 2. **Effect of soluble quenchers on the Tat Trp fluorescence.** 2 μM Tat in citrate buffer, at pH 7.0 or pH 5.3, received the indicated concentration of quencher. F_0/F is the ratio of fluorescence intensity in the absence of quencher (F_0) to the intensity in the presence of quencher (F), against the quencher concentration. *A,* quenching by I^-; *B,* quenching by Cs^{2+}; *C,* quenching by acrylamide. Representative results of triplicate experiments are presented. Similar data were obtained using a phosphate buffer.

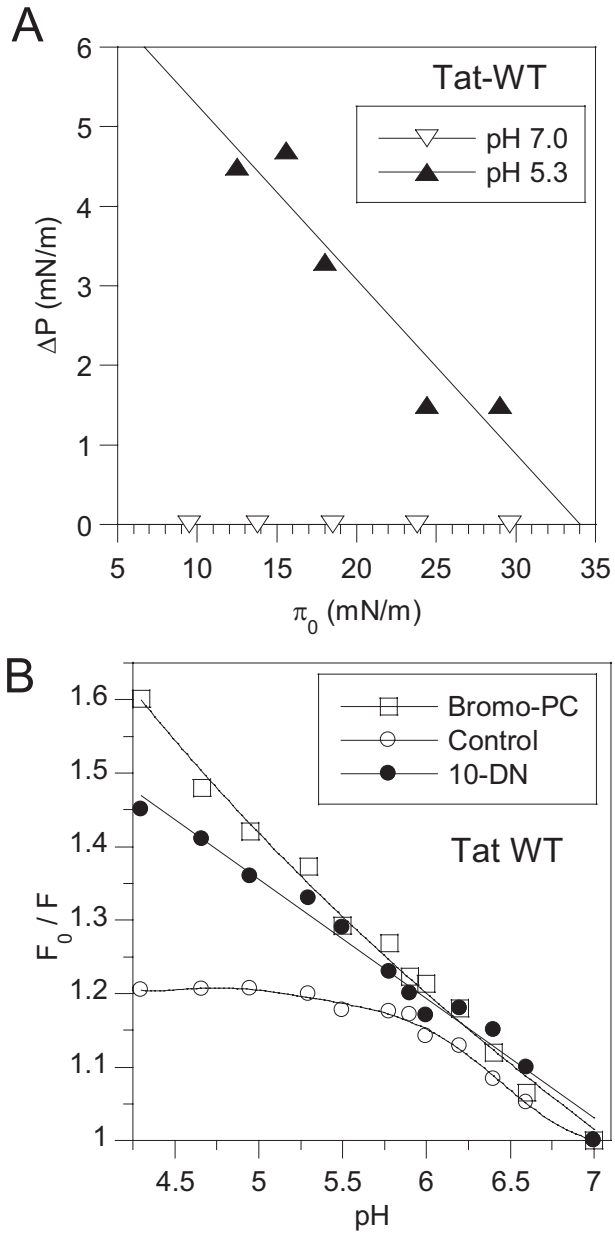

FIGURE 3. **Tat inserts into model membranes upon acidification.** *A,* monolayer penetration of Tat. Tat insertion into monolayers was monitored using $\Delta\pi$ as a function of π_0. Monolayers were made of PC/PG (75/25), and the subphase was citrate buffer at the indicated pH and contained 26 nM Tat. Each point represents an independent experiment. Statistical significance calculated using the correlation coefficient test is $p < 0.02$ for pH 5.3 and $p < 0.001$ for pH 7.0. *B,* quenching of Tat Trp fluorescence by lipid vesicles. Tat (2 μM) was quickly mixed with lipid vesicles composed of PC/PG (75/25; *Control*), PC/bromo-PC/PG (37.5/37.5/25; *bromo-PC*), or PC/PG/10-DN (75/25/10; *10-DN*) in citrate buffer. F_0/F is the ratio of fluorescence intensity at pH 7.0 relative to that at the indicated pH. Shown are representative results of triplicate fluorescence experiments.

after Tat injection into the subphase. Extrapolation of the $\Delta\pi$ *versus* π_0 plot yields π_C, the highest π_0 pressure of a monolayer that a protein can penetrate (38). Fig. 3*A* shows that, at neutral pH, Tat does not penetrate monolayers, regardless of π_0. Nevertheless, acidification to pH 5.3 following Tat injection

induced membrane penetration with π_C in the 30–35 mN/m range. Because the surface pressure of biological membranes and large unilamellar vesicles has also been estimated at 30–35 mN/m, this result indicates that Tat can penetrate model and biological membranes at pH 5.3, hence at endosomal pH (40).

Tat Trp Inserts into Model Membranes upon Acidification—If Tat is able to insert into model membranes upon acidification, and if Trp-11 is significantly involved in this insertion process, it should directly contact lipids and therefore be accessible to membrane-embedded quenchers such as dibromo-PC (24) or 10-doxylnonadecane (10-DN) (36). In the presence of control lipid vesicles, some Tat Trp quenching took place during acidification, but this quenching was relatively weak and plateaued below pH 5.7 (Fig. 3*B*), contrary to what was observed in the absence of membrane, where an almost linear relationship between acidification and quenching was observed (Fig. 1*A*). This difference indicated that Tat Trp environment changed in the presence of vesicles. Moreover, quenching efficiency below pH 6 was strongly enhanced by the presence of brominated PC or 10-DN into the vesicles (Fig. 3*B*), showing that Tat Trp inserts into liposomes at low pH. Within the endosome pH range (pH 5–7), both quenchers were equally efficient at quenching Tat Trp.

Mutation of Tat Trp Does Not Impair Transactivation or Endocytosis—To investigate the role of Tat Trp in membrane insertion and translocation in more detail, we replaced it by another aromatic residue (Phe or Tyr) or a hydrophobic residue (Leu or Ala). The respective abilities of these residues to insert into membranes is Trp ≫ Phe >Tyr > Leu ≫ Ala (41). We first assessed whether these mutations significantly modified the Tat structure. To this end, we monitored the transactivation activity of cytosolically expressed mutants. This assay indeed requires Tat interaction with several partners (proteins and RNA) (25), involves several domains of the protein, and highlights structural modifications. For this assay, Tat and luciferase vectors were cotransfected into Jurkat cells, and transactivation activity was measured after 48 h. Tat-W11F and Tat-W11L transactivated less efficiently than native Tat, indicating that these mutations altered Tat structure and reactivity (Fig. 4). The W11A mutation had already been reported as not affecting Tat transactivation activity (25).

We then used immunofluorescence to assess whether Trp mutants were efficiently recognized and internalized by T-cells, one of the main Tat targets (15). None of the Trp-11 mutations affected endocytosis efficiency (Fig. 5, *A* and *B*). Regarding intracellular routing, we previously found that, upon uptake by T-cells, Tat concentrates within late endosomes, although a minor fraction (10–20%) remains within early endosomes (15). Just like native Tat, all the Trp-11 mutants accumulated within Lamp-1-positive late endosomal structures, whereas 15–20% were present in Tf-positive early endosomes (Fig. 5, *A* and *C*). We concluded that, even though Tat-W11F and Tat-W11L structures seemed modified, none of the Tat Trp mutations significantly affected Tat endocytosis efficiency and intracellular routing.

Implication of Tat Trp in Acid-triggered Membrane Insertion—We then examined the role of Tat Trp in membrane insertion using these Trp mutants. We used membrane monolayers because the use of Trp fluorescence was not possible in that case. As illustrated in Fig. 6, at neutral pH, only background insertion was observed (Δp <1 mN/m) for all mutants. Hence, Trp mutation did not affect the low-pH sensor of the molecule that prevented membrane insertion at neutral pH. When pH was lowered to pH 5.3, Tat-W11Y and Tat-W11F inserted into the monolayer with π_C in the 30–35 mN/m range (Fig. 6), as observed for native Tat (Fig. 3*A*). Tat-W11A and Tat-W11L did not penetrate the membrane at any pH (Fig. 6). Hence, an aromatic residue in position 11 is required for acid-triggered Tat membrane insertion.

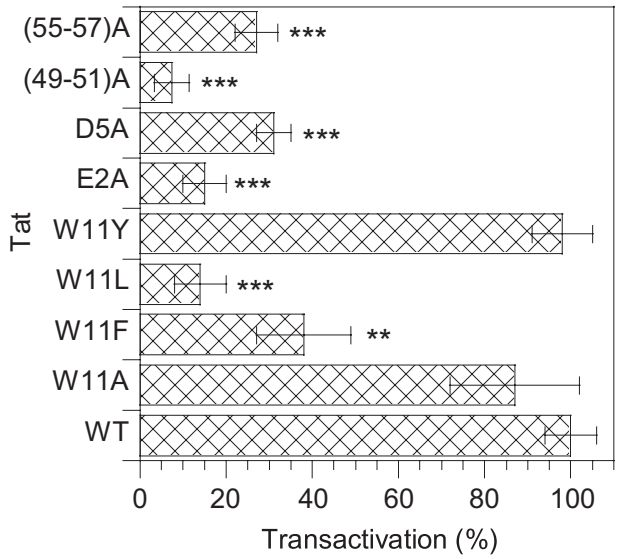

FIGURE 4. **Transactivation activity of transfected Tat mutants.** This assay enabled evaluation of proper Tat folding and reactivity. Cells were cotransfected with a Tat-expressing plasmid together with two luciferase reporter vectors. The first one encoded a firefly luciferase gene under the control of a Tat-activated promoter (*i.e.* HIV-1-LTR), and the other encoded a *Renilla* luciferase gene under the control of a Tat-independent promoter. Luciferase activities were assayed 48 h later, and transactivation was calculated using the firefly/*Renilla* activity ratio (15). Data are means of two independent experiments performed in quadruplicate ± S.E. The significance of differences with native Tat was assessed using an unpaired, two-sided Student's *t* test (***, $p < 0.001$; **, $p < 0.01$). *WT*, wild type.

Tat Trp Is Required for Tat Endosomal Translocation—The next step was to use biological membranes and assess the role of Tat Trp in translocation across the endosome membrane. We previously characterized this translocation process in some detail using a cell-free translocation assay based on the use of ^{125}I-Tat (15). This assay could not be used with Tat Trp mutants because they were not radiolabeled with the same efficiency, and this process led to inactivation of Tat-W11A (supplemental Table 1). To circumvent this difficulty, we used a transactivation assay in which recombinant Tat Trp-11 mutants were added to the medium of luciferase-transfected cells. Indeed, all mutants were endocytosed with an efficiency similar to that of native Tat (Fig. 5), and once in the cytosol, with the exception of Tat-W11F and Tat-W11L, they transactivated just as well as native Tat (Fig. 4). Measuring the transactivation efficiency of exogenous recombinant Tat Trp-11 mutants should thus enable evaluation of their translocation activity. Surprisingly, extracellular Tat-W11A was able to transactivate, but this mutant produced poorly reproducible results in this assay (Fig. 7); this might have been due to poor stability in the

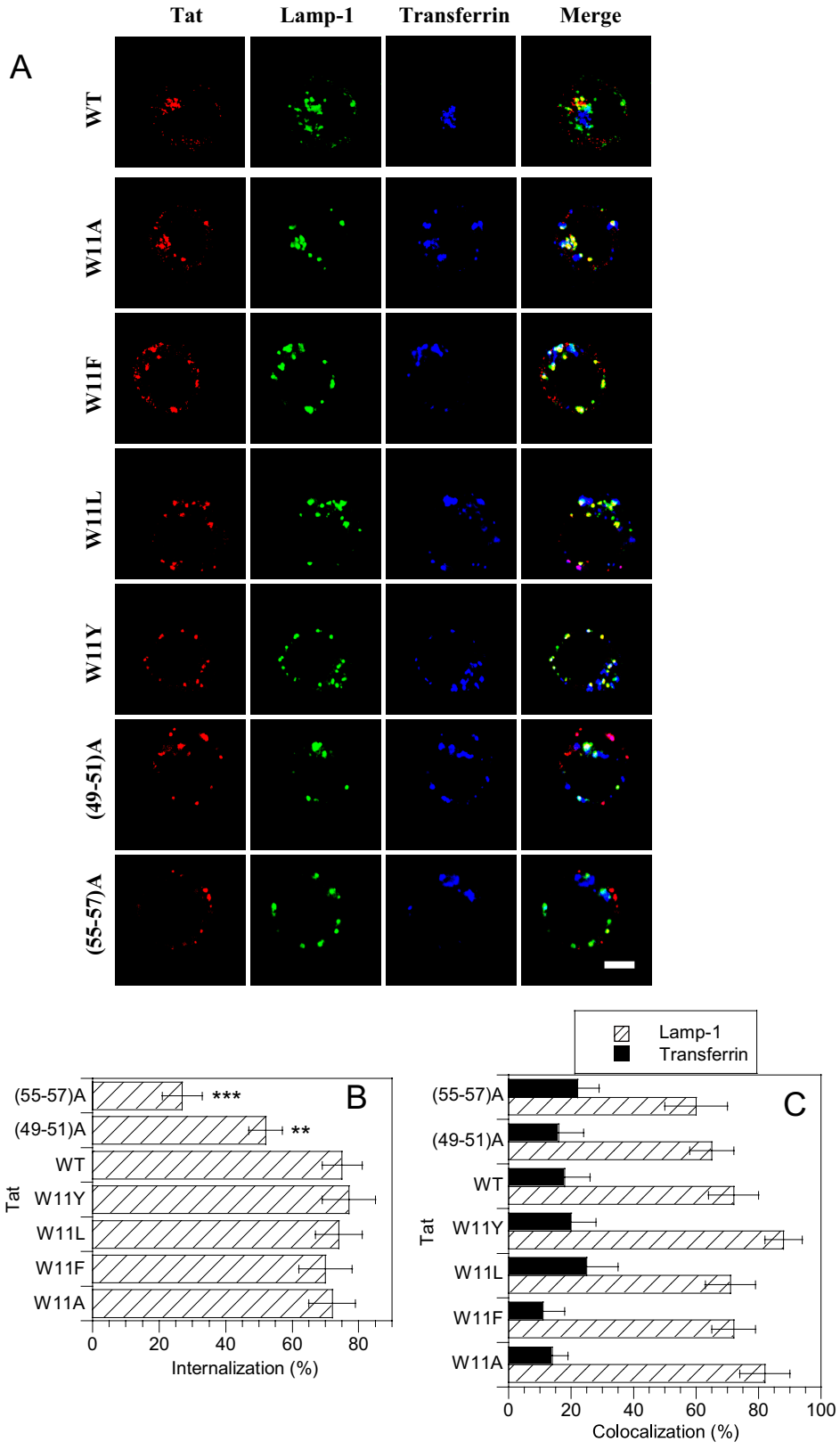

FIGURE 5. **Endocytosis efficiency and intracellular routing of Tat mutants.** Jurkat cells were incubated with 50 nM Tat (or mutant) for 6 h, and Tf-Cy5 was added for the last 40 min. Cells were then washed, fixed, and permeabilized for detection of Tat and Lamp-1 by immunofluorescence. *A,* median optical sections were recorded using a confocal microscope. *Bar,* 5 μm. *WT*, wild type. *B,* images from 20 to 30 cells were recorded, and the endocytosis efficiency was determined as described under "Experimental Procedures." *C,* colocalization of Tat with Lamp-1 and transferrin was calculated using images from 20 to 30 cells and the Metamorph software. The significance of differences with native Tat assessed by Student's *t* test is indicated (***, $p < 0.001$; **, $p < 0.02$). None of the mutations significantly modified Tat intracellular distribution.

extracellular medium, as already indicated by inactivation upon ^{125}I incorporation (supplemental Table 1). This mutant also showed unspecific membrane binding when expressed intracellularly (data not shown), indicating that it interacted nonspecifically with membrane proteins. The other Trp-11 mutants transactivated with efficiency below 25% that of native Tat (Fig. 7). This was not surprising in the case of Tat-W11F and Tat-W11L that have very low intrinsic transactivation capacity (Fig. 4).

The case of Tat-W11Y was the most interesting. This mutant transactivated properly (Fig. 4), indicating that it retained Tat native folding. It was correctly endocytosed and efficiently routed to late endocytic structures intracellularly (Fig. 5). It was able to insert into model membranes upon acidification to endosomal pH (Fig. 6), but when added outside the cell, it hardly reached the cytosol (Fig. 7). We concluded that, although other aromatic residues such as Phe or Tyr can replace Trp to ensure low pH-induced membrane insertion (Fig. 6), this is not the case for the entire translocation process that requires Tat Trp at a stage beyond insertion.

Tat Basic Domain Is Required for Efficient Membrane Insertion—The Tat basic domain (residues 49–57) is able to vectorize cargo proteins into cells (28), so it was important to examine the contribution of this domain in Tat entry. We prepared two Tat mutants, Tat(49–51)A and Tat(55–57)A, that both lack three positive charges within this domain. It is well established that Tat basic domain confers TAR RNA binding properties to Tat (25), and it was therefore not surprising to find that Tat(55–57)A and especially Tat(49–51)A had low transactivation capacities (Fig. 4). It is difficult in that case to draw any conclusion regarding structure preservation because mutations directly affected a region involved in RNA binding. These basic domain mutants were endocytosed less efficiently than

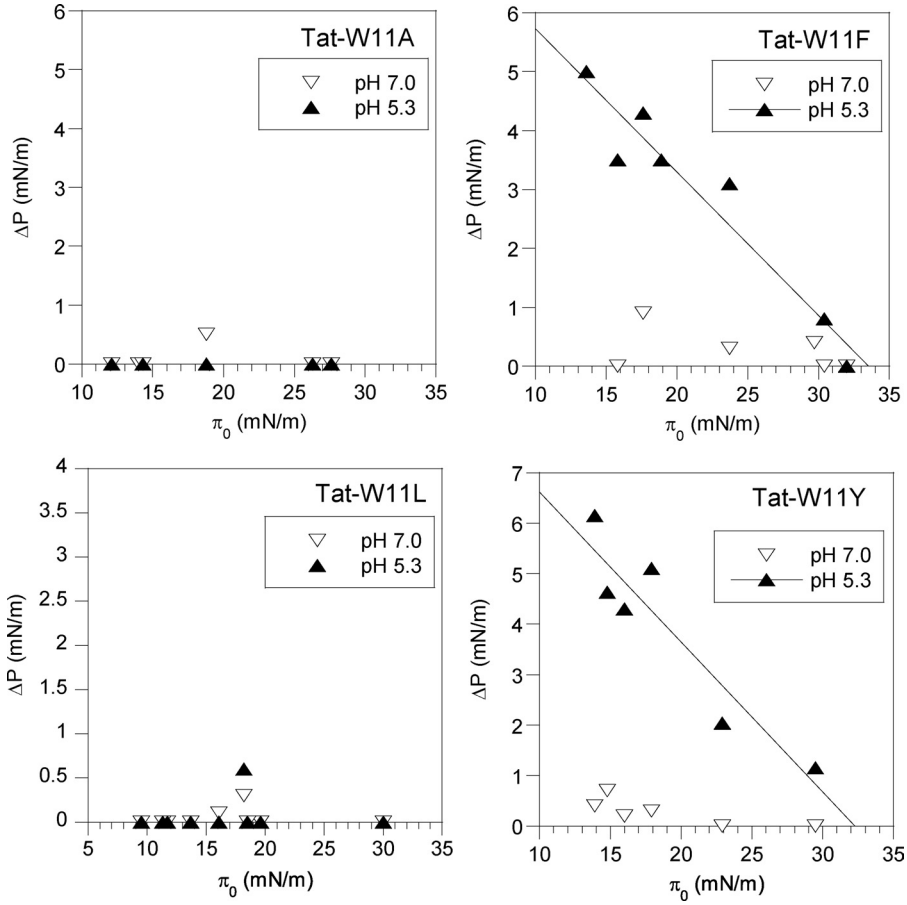

FIGURE 6. **Monolayer penetration of Tat Trp mutants.** Insertion was monitored using $\Delta\pi$ as a function of π_0. Monolayers were made of PC/PG (75/25). The subphase was citrate buffer at the indicated pH and contained 26 nM Tat mutant. Each point represents an independent experiment. Only statistically significant linear regressions were plotted. This significance is $p < 0.001$ and $p < 0.01$ for the insertion at pH 5.3 of Tat-W11F and Tat-W11Y, respectively.

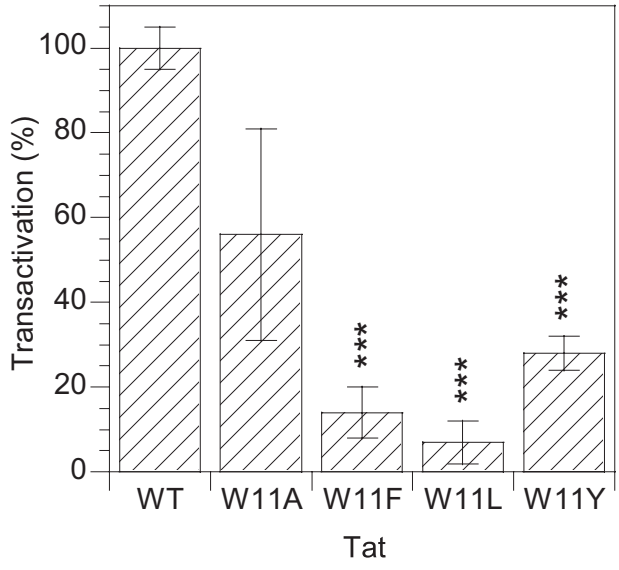

FIGURE 7. **Transactivation activity of exogenous Tat Trp mutants.** Cells were transfected with the luciferase reporter vectors. After 1 day, 200 nM recombinant Tat or mutant and 100 μM chloroquine were added. Luciferase activities were assayed 48 h later, and transactivation is expressed as percentage of wild type (*WT*) Tat activity. Data are mean of two independent experiments performed in quadruplicate ± S.E. The significance of differences with native Tat was assessed using a Student's *t* test (***, $p < 0.001$).

native Tat, and especially for Tat(55–57)A, a large fraction remained at the plasma membrane (Fig. 5, *A* and *B*). This finding indicates that the basic domain is required for efficient Tat uptake. The (49–51)A and (55–57)A mutants followed the same intracellular pathway as native Tat (Fig. 5*C*).

We then assessed whether Tat basic domain mutants could insert into model membranes upon acidification. We used lipid vesicles and membrane-embedded quenchers, distearoylbromo-PC, which bears bromide atoms in positions 9 and 10, and 10-DN, which is a highly hydrophobic molecule containing a nitroxide and that is thought to distribute homogeneously within the membrane core (36). The resulting quenching curves (Fig. 8, *top panels*) were strikingly different from that of native Tat (Fig. 3*B*). Compared with control vesicles, brominated liposomes poorly affected mutant fluorescence, showing that these mutants, especially Tat(49–51)A, failed to insert deeply into the membrane. Nevertheless, Tat(55–57)A fluorescence was very efficiency quenched by 10-DN, indicating that this mutant superficially inserted into the membrane (Fig. 8). This was also observed for Tat(49–51)A but to a much lower extent. These findings were confirmed by monolayer insertion results. Indeed, Tat(49–51)A did not significantly insert into monolayers whatever the pH (Fig. 8, *bottom panels*), whereas Tat(55–57)A inserted efficiently at acidic pH (π_0 = 30–35 mN/m) and, interestingly, inserted weakly but significantly at neutral pH (π_0 = 22–26 mN/m). We will come back to this point below. These combined insertion data show that, upon acidification, Tat(49–51)A membrane penetration is weak and superficial, whereas Tat(55–57)A inserts much more efficiently. Nevertheless, Tat(55–57)A does not seem to insert as deeply into the membrane as native Tat.

Glu/Asp-2 and Tat Basic Domain Constitute a Low pH Sensor That Regulates Tat Membrane Insertion—Because Tat only inserts into the membrane below pH 6.0 (Fig. 3), a pH sensor device should be present to prevent Trp exposure above this pH. An interesting candidate to fulfill this role was the strong interaction between acidic N-terminal residues and positively charged residues in the basic domain (35, 42). Indeed, protonation of the carboxyl of the Glu/Asp side chain upon acidification would likely destabilize this electrostatic interaction and open the Tat structure. If a charged residue plays a role in low-pH sensing, its replacement by a neutral residue should allow membrane insertion at pH values above those required to

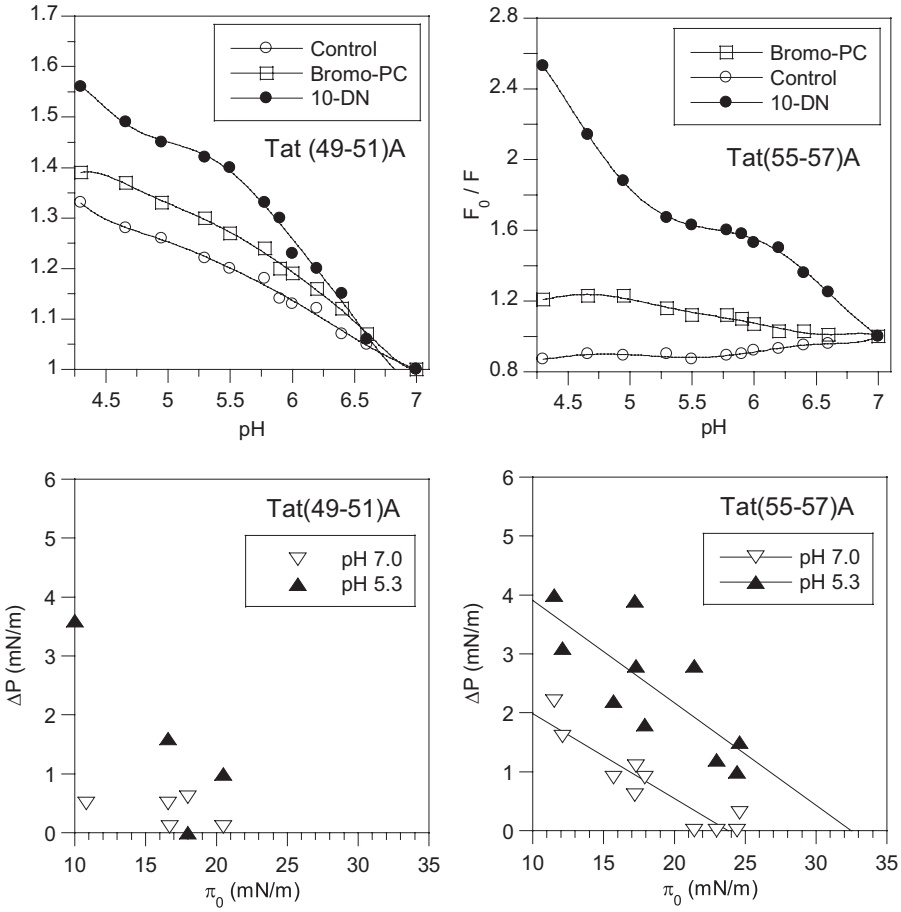

FIGURE 8. **Membrane insertion of Tat basic domain mutants.** *Upper panels,* quenching of mutant Trp fluorescence by lipid vesicles. *Lower panels,* monolayer penetration of Tat basic domain mutants. Experiments were performed as described in the legend to Fig. 3. The statistical significance of the linear regressions is $p < 0.01$ for Tat(55–57)A at pH 5.3 and $p < 0.001$ at pH 7.0.

ensure membrane insertion of native Tat. This is exactly what was observed using Tat(55–57)A that, contrary to Tat(49–51)A, inserted significantly into membrane monolayers at neutral pH (Fig. 8). To confirm these findings, we monitored, using Trp fluorescence, mutant insertion into liposomes at mildly acidic pH (pH 6–7). We focused on the initial steps of membrane penetration using vesicles containing 10-DN, so that we could detect Trp side chain insertion as soon as it entered the hydrophobic part of the membrane. Under these conditions, no insertion of native Tat or Tat(49–51)A could be detected using 10-DN (Fig. 9). Nevertheless, Tat(55–57)A fluorescence exhibited enhanced susceptibility to 10-DN quenching as soon as the pH dropped below pH 6.7. This result indicates that Tat(55–57)A lost the low-pH sensor that regulates Tat insertion and that the Arg triplet 55–57 belongs to this sensor. Because the Tat basic domain stays in an extended conformation and exhibits a lot of flexibility (31, 42), we did not attempt to identify the residue, if any, within this triplet that would be more specifically interacting with acidic N-terminal residues.

We then tried to identify this or these negative residue(s). To this end, we mutated Glu-2 and Asp-5 to Ala and examined the capacity of the corresponding mutants to insert into membranes. Although Tat-D5A inserted poorly into membrane monolayers at low pH (π_0 = 25–27 mN/m) and not significantly at neutral pH, Tat-E2A inserted efficiently at acidic pH (π_0 = 30–32 mN/m) and significantly at neutral pH (π_0 = 26–30 mN/m) (Fig. 10). This indication that Glu/Asp-2 belongs to the low-pH sensor was confirmed using Trp fluorescence and liposomes. Interestingly, although Tat-D5A like native Tat did not insert into liposomes above pH 6, Tat-E2A inserted just as efficiently as Tat(55–57)A (Fig. 9). Hence, the Tat low-pH sensor involves Glu-2 and the Arg triplet 55–57. Trp fluorescence of the corresponding mutants specifically showed enhanced susceptibility to acrylamide quenching at neutral pH (data not shown), indicating that inactivation of the Tat low-pH sensing device results in increased exposure of Trp-11 to the outside of the molecule at neutral pH. Finally, it should be noted that the poor intrinsic transactivation activity of acidic and basic domain mutants (Fig. 4) prevented examination of their translocation activity using recombinant proteins added to reporter gene-transfected cells.

DISCUSSION

HIV-1 Tat is notoriously refractory to crystallization, and published structural studies were based on two-dimensional NMR experiments. Despite the high positive charge density and the paucity of hydrophobic residues, a conformation was obtained using an 86-residue version of Tat at mildly acidic pH (pH 6.3–6.5 (31)). Molecular dynamics simulations indicated that this conformation exhibits a high degree of flexibility. Tat is nevertheless stabilized by interactions between the acidic N-terminal domain and the basic domain of the protein (39). A different conformation was observed at acidic pH (pH 4.1–4.5) using a similar 86-residue Tat (43). Regardless of whether these conformations are stable, transient, or molten globule-like, it seems that Trp-11 is poorly accessible to the solvent at mildly acidic pH (31) but is much more exposed to the outside at low pH (43). Moreover, a molecular dynamics analysis of a reduced version of Tat (residues 1–72) at pH 4.1 suggests that this truncated Tat is unfolded at low pH (44).

Here we used different Trp fluorescence quenchers and found that, in agreement with the findings of structural studies (31, 43, 44), Tat Trp becomes exposed upon acidification. Consistent with cell-based results showing that Tat translocates through the endosome membrane (15), we observed that acidification induced Tat insertion into model membranes such as monolayers or SUV. This insertion process requires an aromatic residue at position 11 of the protein because Tat Trp-11

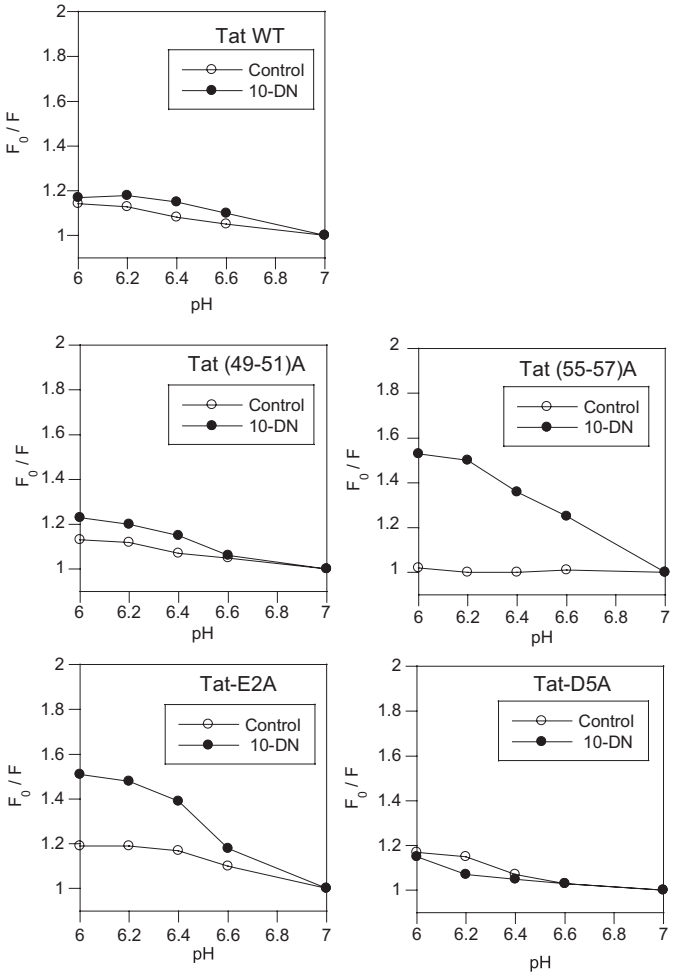

FIGURE 9. **Insertion of Tat mutants into lipid vesicles at mildly acidic pH.** Tat or the indicated mutant (2 μM) was added to lipid vesicles composed of PC/PG (*Control*) or PC/PG/10-DN (*10-DN*) in citrate buffer. F_0/F is the ratio of fluorescence intensity at pH 7.0 relative to that at the indicated pH. Representative results of triplicate experiments are shown. *WT*, wild type.

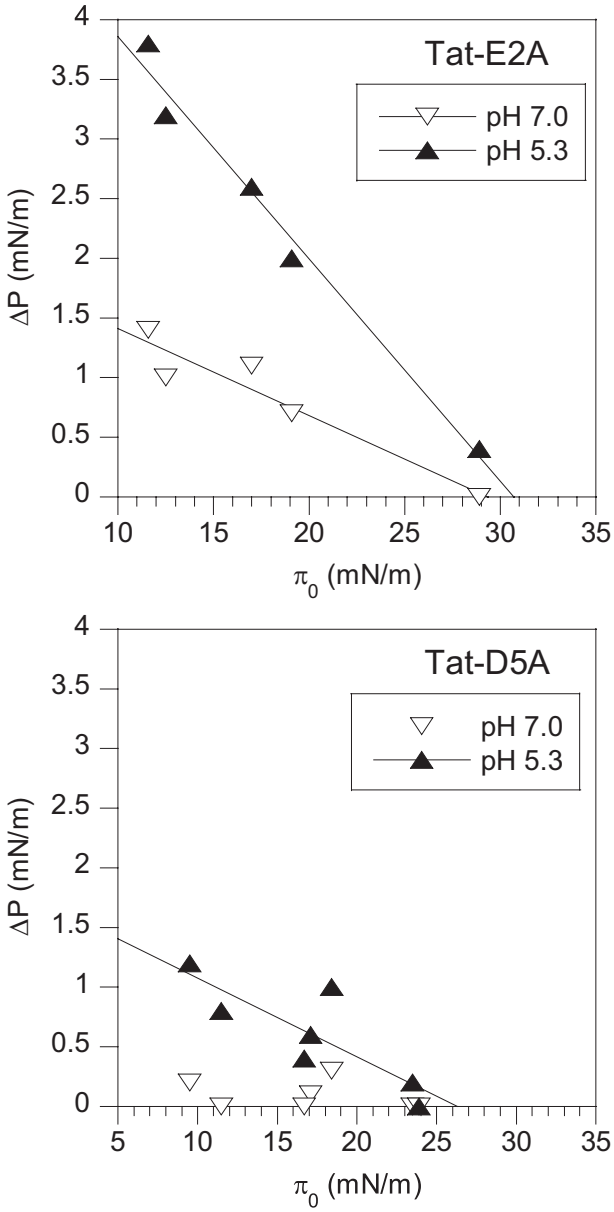

FIGURE 10. **Monolayer penetration of Tat acidic domain mutants.** Experiments were performed as described in the legend to Fig. 3. The statistical significance of the linear regressions is $p < 0.01$ for Tat-E2A at pH 5.3 and $p < 0.02$ for Tat-E2A at pH 7.0. For Tat-D5A it is $p < 0.02$ at pH 5.3.

could be replaced by Phe or Tyr but not by Leu or Ala. Nevertheless, when the entire translocation process was examined, Trp-11 was strictly needed, and no other hydrophobic residues could replace it. This finding is consistent with the conservation of this residue among Tat from different viral isolates (35). Studies of the third helix of Antennapedia, a *Drosophila* homeodomain that is able to reach the cell cytosol from the outside, also identified a key Trp residue that is required for translocation and could not be replaced by Phe (45).

We showed here that Tat uses a Trp-mediated regulated membrane insertion process, as described previously for other proteins such as annexin-V (32), protein kinase C-α (33), and PEA (24). In the case of PEA and Tat, the stimulus leading to Trp exposure and membrane insertion is acidification, and it was therefore interesting to examine whether a low-pH sensor system such as the one identified in PEA could also be found in Tat. Indeed, low pH is detected by PEA-Asp-358 that is, at neutral pH, engaged in an H-bond that is destabilized when the Asp-carboxyl becomes protonated at pH < 5.5. This will eventually trigger Trp-305 exposure (24).

We looked for Tat residues that could potentially be involved in low-pH detection and induced Trp side chain exposure and membrane insertion at endosomal pH. Strong candidates were acidic residues from the N-terminal domain that is connected to the basic domain by electrostatic interactions that stabilize the molecule. These residues are Asp-2 or Glu-2 depending on viral isolates, Asp-5 and Glu-9 (39, 42). They are well preserved among viral isolates but, compared with the others, Asp/Glu-2 establishes more stabilizing H-bonds with the basic domain (39, 42). In agreement with structural studies (39), we found that Glu-2, but not Asp-5, is involved in low-pH sensing by Tat and that the E2A mutation enables Tat membrane insertion above pH 6. Low-pH sensing by Tat is most likely due to a pH-sensitive H-bond between Asp/Glu-2 and the end of the basic domain, because mutation of the 55–57 Arg triplet recapitulated the Tat-E2A membrane insertion phenotype (Figs. 8–10).

The fact that some Trp-11 mutants such as Tat-W11A and Tat-W11Y retained complete transactivation activity indicated that they preserved a native conformation that enables them to interact with the different partners involved in this activity. Although other mutations decreased transactivation activity, it should be noted that informative mutants such as Tat-W11F and those corresponding to the low-pH sensor (Tat-E2A and Tat(55–57)A) nevertheless retained their capacity to insert into membranes upon acidification (Figs. 6, 8, and 10). Hence, they are not too drastically affected in their conformation and conserved, at least partially, Tat capacity to achieve low pH-induced membrane insertion.

In addition to its role in low-pH sensing, we found that the Tat basic domain is required for efficient membrane insertion, because a much shallower insertion was observed when three positive charges were removed from this domain (Fig. 8). Tat-PTD positive charges are likely necessary to achieve efficient Tat binding to the phosphate groups of bilayer phospholipids (46), so that efficient Trp insertion into the membrane core can take place. Removing positive charges from the basic domain also inhibited Tat endocytosis (Fig. 5, *A* and *B*). Hence, the basic domain is involved in three key steps of Tat entry into cells as follows: endocytosis, low-pH sensing, and membrane insertion. The two halves of the domain do not contribute equally to these processes, the N-terminal portion being more specifically needed for membrane insertion, and the C-terminal part is more important for endocytosis and ensures low-pH sensing together with Glu/Asp-2. The implication of the basic domain in Tat endocytosis and membrane insertion is consistent with the ability of Tat-PTD to act as a vehicle to vectorize cargos such as proteins or DNA to the cell cytosol (28). Nevertheless, although Tat and its PTD share the same receptors (18, 26) and can enter cells using clathrin-mediated endocytosis (15, 28), the PTD lacks Tat Trp. Our results showing that Tat-W11A was unable to insert into membrane monolayers at any pH and initial pressure (Fig. 6) are consistent with the fact that, to our knowledge, Tat-PTD has not been found to penetrate model membranes. Interestingly, attaching a Trp to Tat-PTD does enable insertion into model membranes (47), and hooking a Trp to Tat-PTD or other PTDs should thus increase the efficiency of cargo cytosolic delivery. In agreement with the absence of a low-pH sensor in Tat-PTD, membrane insertion of the Trp-Tat-PTD peptide was found to take place at neutral pH (47). Regarding the Tat-PTD mechanism of cellular uptake, it is not clear whether Tat-PTD requires low endosome pH to reach the cytosol, because inhibitors of endosomal acidification provided contrasting results with respect to the uptake of fluorescent Tat-PTD (48).

Because mutants such as Tat-W11A and Tat-W11L failed to insert into membranes upon acidification, it seems clear that Tat insertion is initiated by Trp-11. Other well preserved hydrophobic residues such as Phe-38 or Leu-43 (35) within the core domain are likely involved in membrane insertion and/or translocation but acting downstream of Trp-11.

Acidic residues are involved in low-pH sensing by several bacterial toxins such as colicin (49), botulinum (50), and diphtheria toxin (51) where Asp or Glu are found in key positions (49–51). Nevertheless, membrane insertion of these toxins is thought to rely on translocation domain hydrophobic segments. Hence, the Tat membrane insertion process is mechanistically closer to that of PEA (24). These two toxins indeed use an acidic residue as pH sensor and a Trp side chain for membrane penetration. HIV-1 Tat thus uses molecular tricks similar to those developed by an unrelated bacterial toxin to achieve endosomal escape to the cytosol. The finding that Tat Trp is specifically required for endosomal translocation together with the observation that, despite the high HIV-1 mutation rate (34), this Trp is conserved between viral isolates (35) indicates that the ability of Tat to cross membranes is important for HIV-1 multiplication.

Acknowledgments—We are indebted to Erwin London for the kind gift of 10-DN; Laurent Chiche, Christian Roy, Gilles Divita, and Paolo Carloni for discussions; Teresa Alvarez for assistance during Tat purification; and Reza Gholizadeh, Manon Gérard-Vincent, and Jocelyn Méré for help in the pioneer experiments.

REFERENCES

1. Huigen, M. C., Kamp, W., and Nottet, H. S. (2004) *Eur. J. Clin. Invest.* **34,** 57–66
2. Strebel, K. (2003) *AIDS* **17,** Suppl. 4, S25–S34
3. Ensoli, B., Barillari, G., Salahuddin, S. Z., Gallo, R. C., and Wong-Staal, F. (1990) *Nature* **345,** 84–86
4. Rubartelli, A., Poggi, A., Sitia, R., and Zocchi, M. R. (1998) *Immunol. Today* **19,** 543–545
5. Gallo, R. C. (1999) *Proc. Natl. Acad. Sci. U.S.A.* **96,** 8324–8326
6. King, J. E., Eugenin, E. A., Buckner, C. M., and Berman, J. W. (2006) *Microbes Infect.* **8,** 1347–1357
7. Wu, R. F., Ma, Z., Myers, D. P., and Terada, L. S. (2007) *J. Biol. Chem.* **282,** 37412–37419
8. Chang, H. C., Samaniego, F., Nair, B. C., Buonaguro, L., and Ensoli, B. (1997) *AIDS* **11,** 1421–1431
9. Nickel, W. (2005) *Traffic* **6,** 607–614
10. Temmerman, K., Ebert, A. D., Müller, H. M., Sinning, I., Tews, I., and Nickel, W. (2008) *Traffic* **9,** 1204–1217
11. Xiao, H., Neuveut, C., Tiffany, H. L., Benkirane, M., Rich, E. A., Murphy, P. M., and Jeang, K. T. (2000) *Proc. Natl. Acad. Sci. U.S.A.* **97,** 11466–11471
12. Albini, A., Soldi, R., Giunciuglio, D., Giraudo, E., Benelli, R., Primo, L., Noonan, D., Salio, M., Camussi, G., Rockl, W., and Bussolino, F. (1996) *Nat. Med.* **2,** 1371–1375
13. Ensoli, B., Fiorelli, V., Ensoli, F., Cafaro, A., Titti, F., Buttò, S., Monini, P., Magnani, M., Caputo, A., and Garaci, E. (2006) *AIDS* **20,** 2245–2261
14. Ott, M., Emiliani, S., Van Lint, C., Herbein, G., Lovett, J., Chirmule, N., McCloskey, T., Pahwa, S., and Verdin, E. (1997) *Science* **275,** 1481–1485
15. Vendeville, A., Rayne, F., Bonhoure, A., Bettache, N., Montcourrier, P., and Beaumelle, B. (2004) *Mol. Biol. Cell* **15,** 2347–2360
16. Rayne, F., Vendeville, A., Bonhoure, A., and Beaumelle, B. (2004) *J. Virol.* **78,** 12054–12057
17. Gutheil, W. G., Subramanyam, M., Flentke, G. R., Sanford, D. G., Munoz, E., Huber, B. T., and Bachovchin, W. W. (1994) *Proc. Natl. Acad. Sci. U.S.A.* **91,** 6594–6598
18. Tyagi, M., Rusnati, M., Presta, M., and Giacca, M. (2001) *J. Biol. Chem.* **276,** 3254–3261
19. Liu, Y., Jones, M., Hingtgen, C. M., Bu, G., Laribee, N., Tanzi, R. E., Moir, R. D., Nath, A., and He, J. J. (2000) *Nat. Med.* **6,** 1380–1387
20. Frankel, A. D., and Pabo, C. O. (1988) *Cell* **55,** 1189–1193
21. Mann, D. A., and Frankel, A. D. (1991) *EMBO J.* **10,** 1733–1739
22. Falnes, P. O., and Sandvig, K. (2000) *Curr. Opin. Cell Biol.* **12,** 407–413
23. Rosconi, M. P., and London, E. (2002) *J. Biol. Chem.* **277,** 16517–16527
24. Méré, J., Morlon-Guyot, J., Bonhoure, A., Chiche, L., and Beaumelle, B. (2005) *J. Biol. Chem.* **280,** 21194–21201

25. Jeang, K. T., Xiao, H., and Rich, E. A. (1999) *J. Biol. Chem.* **274,** 28837–28840
26. Soane, L., and Fiskum, G. (2005) *J. Neurochem.* **95,** 230–243
27. Ziegler, A., and Seelig, J. (2004) *Biophys. J.* **86,** 254–263
28. Lindgren, M., Hällbrink, M., Prochiantz, A., and Langel, U. (2000) *Trends Pharmacol. Sci.* **21,** 99–103
29. Wadia, J. S., Stan, R. V., and Dowdy, S. F. (2004) *Nat. Med.* **10,** 310–315
30. Richard, J. P., Melikov, K., Vives, E., Ramos, C., Verbeure, B., Gait, M. J., Chernomordik, L. V., and Lebleu, B. (2003) *J. Biol. Chem.* **278,** 585–590
31. Bayer, P., Kraft, M., Ejchart, A., Westendorp, M., Frank, R., and Rösch, P. (1995) *J. Mol. Biol.* **247,** 529–535
32. Campos, B., Mo, Y. D., Mealy, T. R., Li, C. W., Swairjo, M. A., Balch, C., Head, J. F., Retzinger, G., Dedman, J. R., and Seaton, B. A. (1998) *Biochemistry* **37,** 8004–8010
33. Medkova, M., and Cho, W. (1999) *J. Biol. Chem.* **274,** 19852–19861
34. Walker, B. D., and Burton, D. R. (2008) *Science* **320,** 760–764
35. Pantano, S., and Carloni, P. (2005) *Proteins* **58,** 638–643
36. Caputo, G. A., and London, E. (2003) *Biochemistry* **42,** 3265–3274
37. Jiang, J. X., and London, E. (1990) *J. Biol. Chem.* **265,** 8636–8641
38. Stahelin, R. V., Long, F., Peter, B. J., Murray, D., De Camilli, P., McMahon, H. T., and Cho, W. (2003) *J. Biol. Chem.* **278,** 28993–28999
39. Pantano, S., Tyagi, M., Giacca, M., and Carloni, P. (2004) *Eur. Biophys. J.* **33,** 344–351
40. Rodríguez, M., Torrent, G., Bosch, M., Rayne, F., Dubremetz, J. F., Ribó, M., Benito, A., Vilanova, M., and Beaumelle, B. (2007) *J. Cell Sci.* **120,** 1405–1411
41. White, S. H., and Wimley, W. C. (1999) *Annu. Rev. Biophys. Biomol. Struct.* **28,** 319–365
42. Pantano, S., Tyagi, M., Giacca, M., and Carloni, P. (2002) *J. Mol. Biol.* **318,** 1331–1339
43. Péloponèse, J. M., Jr., Grégoire, C., Opi, S., Esquieu, D., Sturgis, J., Lebrun, E., Meurs, E., Collette, Y., Olive, D., Aubertin, A. M., Witvrow, M., Pannecouque, C., De Clercq, E., Bailly, C., Lebreton, J., and Loret, E. P. (2000) *C. R. Acad. Sci. III* **323,** 883–894
44. Shojania, S., and O'Neil, J. D. (2006) *J. Biol. Chem.* **281,** 8347–8356
45. Derossi, D., Joliot, A. H., Chassaing, G., and Prochiantz, A. (1994) *J. Biol. Chem.* **269,** 10444–10450
46. Herce, H. D., and Garcia, A. E. (2007) *Proc. Natl. Acad. Sci. U.S.A.* **104,** 20805–20810
47. Thorén, P. E., Persson, D., Esbjörner, E. K., Goksör, M., Lincoln, P., and Nordén, B. (2004) *Biochemistry* **43,** 3471–3489
48. Fischer, R., Köhler, K., Fotin-Mleczek, M., and Brock, R. (2004) *J. Biol. Chem.* **279,** 12625–12635
49. Musse, A. A., and Merrill, A. R. (2003) *J. Biol. Chem.* **278,** 24491–24499
50. Lacy, D. B., and Stevens, R. C. (1999) *J. Mol. Biol.* **291,** 1091–1104
51. Ren, J., Sharpe, J. C., Collier, R. J., and London, E. (1999) *Biochemistry* **38,** 976–984